Spectrum of Engineering Sciences
ISSN (e) 3007-3138 (p) 3007-312X Volume 4, Issue 3, 2026

MACHINE VISION APPROACH TO DISCRIMINATE AND CLASSIFY NORMAL AND DISEASE-AFFECTED CROP SEEDS

Hina Shafique[1], Aqsa Khursheed[2], Shafqat Ali[3], Samer Parveen[4], Ghulam Gilanie[*5]

[1,2,*5]*Department of Artificial Intelligence, Faculty of Computing, The Islamia University of Bahawalpur, Pakistan.*
[3,4]*Department of Mathematics, Faculty of Physical and Mathematical Sciences, The Islamia University of Bahawalpur, Pakistan*

[1]hinach1912@gmail.com, [2]aqsakhursheedbwp@gmail.com, [3]shafqat.ali@iub.edu.pk, [4]samerrehman18@gmail.com, [*5]ghulam.gilanie@iub.edu.pk

DOI: https://doi.org/10.5281/zenodo.22044164

Keywords
Machine Vision, Crop Seeds, Normal and Diseased Crop

Article History
Received: 13 January 2026
Accepted: 26 February 2026
Published: 12 March 2026

Corresponding Author: *
Ghulam Gilanie

Abstract

Every grower in the agriculture domain eventually observes the consequences of low-quality seeds, which include weak seedlings, moisture loss, inadequate stands, sluggish sprouting, and combined or ethnically compromised lots. The purpose is to have good quality and quantity crops from a marketing point of view. Selection of right seeds can make it possible. Till now, all this is handled manually, but machine vision approach can result better in this regard. Cotton, Wheat and Corn crops are widely cultivated in southern Punjab as well as throughout the world to produce various consumable and wearable items. Since seeds of these crops are evaluated in many areas with the aims of sowing and further processing, they should be identified in an expedited and accurate manner for the selection of a healthy (normal) seed. In this research activity, an affordable machine vision approach has been investigated to classify normal and diseased crop seeds. The experiments have been performed on the dataset gathered from Pakistan's Bahawalpur Agriculture Research Center. The domain specialists sorted plants that were healthy from those that were afflicted by disease. Several of the best forecast models for classifying seeds as normal and unhealthy for all three crops have been obtained through the investigation of feature sets, feature models, and machine learning classifiers. To adjust the algorithm's variables, tests as well as training sets have been utilized with the K-fold cross-validation method. Resultantly, fast and accurate operations have been adopted to serve agricultural industries. For quantitative assessment of the research work, standard evaluation parameters, accuracy, specificity and sensitivity have been used. The developed system achieved an overall accuracy for cotton as (83.8%), for wheat as (100%) and for corn as (84.0%).

1 Introduction

Crops are very important for organisms and human life. They play a vital role in the ecosystem. The quantity of yield depends upon the quality of the seed and of the soil, which hosts different types of crops. Identification of normal and diseased seeds is a complicated and time-consuming task. Formerly, experienced growers or other workers of this field recognize shape and color of crop seed subjectively [1]. Huge volumes of crop seeds usually cannot be graded manually. So, automatic procedures performing the requisite will be among the more convenient means. Recently, researchers have proposed automated methods to classify normal and disease-affected seeds [2]. A quick and

ISSN (e) 3007-3138 (p) 3007-312X Volume 4, Issue 3, 2026

accurate recognition and identification of normal and disease-affected seeds has worth in the field of agriculture and botany [2]. The use of seeds in different agricultural areas has increased the significance of their proper identification and/or grading. Each seed contains multiple features, which help to identify and classify it as normal or diseased [4]. These features include seed size, dispersal, color and dormancy [3]. Agronomists and other relevant specialists analyze and classify seeds by visually or chemically examining each sample [6]. Although it takes time, it offers crucial information for impurity determination. Consequently, it will be more convenient to have it done instantly [7].

In agriculture environments, farmers usually grade seeds based on their experience. Owing to limited experience, they often grade their seeds erroneously. Mostly, in such cases farmers grade or classify the seeds as per their own experience or previous knowledge [4-7].

If such automated systems performing auto classification and grading of seeds are integrated into available machines used by these farmers or agrarians, no doubt the time and resources both will be saved in efficient manners. Figure 1 shows sample images of different normal and diseased seeds. These images have been obtained from dataset [8], which includes Cotton, Wheat and Corn seeds.

A

B

C

D

E

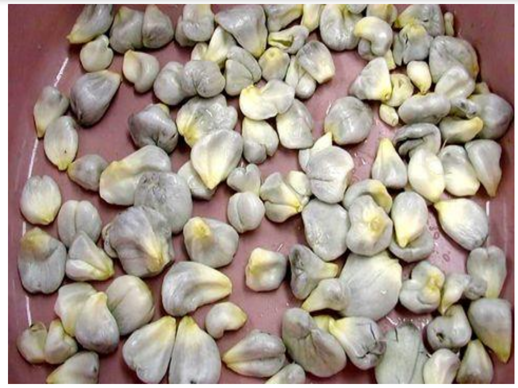

F

Figure 1: Shows normal and diseased seeds of cotton, wheat and corn [8] (A) Shows normal seeds of cotton (B) Shows diseased seeds of cotton (C) Shows normal seeds of wheat (D) Shows diseased seeds of wheat (E) Shows normal seeds of corn (F) Shows diseased seeds of corn [8]

Several investigators have tried to develop a semi-automated/automated system in this research work for the discrimination/identification of different seeds to have their objectives. Some of them are cited below.

The researchers [9] proposed a computer-vision-based method for the classification of castor seeds. They used the two most common seed groups on the images, recorded through a webcam [9-32]. They used frequency distribution for every color channel, i.e., red, green, blue. These investigators have also used hue, saturation, intensity, and grayscale information. Partial least squares-discriminant analysis (PLS-DA) and linear discriminant analysis (LDA) have been used as pattern recognition methods to successfully classify each of the seed classes. They claimed 97.5% and 98.8% classification rates, respectively [33-53].

The authors [54] have registered a US patent, in which an automated system for the analysis of seeds through images has been published. The strategy involves examining tissue removed from the seeds for the presence or absence of at least one characteristic and selecting seeds based on that characteristic.

Another method [55] has been reported in literature for the classification of weed seeds, in which the authors used a Principal Component Analysis (PCA) Network. They validated their results on data sets containing 91 types of weed seeds [56-88].

A technique for the type of pepper seed [89] based on neural networks and computer vision techniques has been reported; images having a resolution of 1200 dpi were used for their experiments. Color, shape, and texture-based features have been extracted and employed to classify pepper seeds. To prevent overfitting, the authors used a cross-validation approach. The reported accuracy rate is 84.94%.

As per reviewed literature, it is concluded that there is a substantial research gap in this area to automatically classify, grade and discriminate healthy and disease-affected seeds. Moreover, the reported approaches are computationally expensive, and the measures they obtain leave room for improvement.

This research investigates the seeds classification based on their texture. In routine, seeds are classified or graded as normal, healthy and diseased based on their visual analysis by domain experts. In most cases, domain experts are agrarians or farmers of expert level. During the last few decades, various methods were suggested for classifying seeds according to the design method and data gathering strategy. These methods are classified as multi-modal, vision-based, and non-visual sensor-based. It is true that seed categorization schemes are complicated and are built up of various components. The purpose of this thesis is to create new methods by utilizing handcrafted and machine learning-based algorithms to classify seeds using a vision-based strategy. The primary goals of this study are:

(a) Discrimination of seeds as normal, healthy and diseased based on their texture.

(b) Develop an automated system which could auto classify seeds in more efficient and definite manners.

(c) Classification of seeds using machine vision approaches.

(d) Development of an automated system for the discrimination of normal and disease-affected seeds; this is a more reliable and standard approach.

(e) Provide an automatic system for the discrimination of healthy seeds.

(f) A thorough analysis of the most advanced methods based on both machine learning and handcrafted approaches to determine which one performs best;

(g) Recognizing the shortcomings of cutting-edge methods and pinpointing areas in need of improvement;

(h) Development of a novel technique for seeds classification, which is considered as one of the major challenges in different application domains of agriculture;

In this study, a machine learning-based approach for classifying seeds from photos has been put forth. The research begins by examining and analyzing the textural properties of seed images in order to identify the seeds as either healthy or unhealthy. The textural properties considered were kurtosis, homogeneity, contrast, entropy, smoothness, and mean. Each training image was convolved with 2D Gabor filters to determine the texture properties of image I(x,y).

2 Literature Review

Categorization of seed varieties has been done by [22]. In that work, the authors assess varietal quality with the aim of improving crop yield through variety classification. To classify the varieties of maize seeds, a hyperspectral imaging system covering the spectral range of 874–1734 nm was used. Their technique assessed a total of 12,900 maize seeds, comprising three distinct types. The 975.01–1645.82 nm bands were retrieved and preprocessed. A radial basis neural network was used to create discriminant models (RBFNN). It was investigated how calibration sample size affected accuracy in classification. The findings indicated that while prediction accuracy changed from an improving form to a stable form as the calibration sample size increased, calibration accuracy varied marginally.

As a result, the ideal calibration set size was established. Principal components (PCs) loading was used to identify the optimal wavelength. With a calibration accuracy of 93.85% and a prediction accuracy of 91.00%, the RBFNN model, which was created on ideal wavelengths and with the ideal size of the calibration set, produced good results. By using this RBFNN model on the average spectra of each sample, a categorization map of seed varieties was produced. Additionally, support vector machines (SVM) were used to validate the process for determining the ideal sample size suggested in this investigation. The overall findings suggested that hyperspectral imaging was a promising method for classifying maize seed varieties and would aid in the creation of a real-time detection system for both maize and other crop seeds.

Studies of a certain plant's visually discernible patterns are referred to as plant trait/disease studies. Crops today deal with a lot of illnesses and characteristics. Insect damage is one of the main characteristics or diseases. Since some types of birds may be poisoned by insecticides, their effectiveness has not always been demonstrated. Additionally, it disrupts the normal animal feeding chains. Using a scale based on the percentage of the afflicted area, plant scientists frequently measure the damage caused by disease to plants (leaves, stems). Low throughput and subjectivity are the outcomes. This work offers developments in a number of techniques for image processing-based plant disease and trait research. The techniques being examined aim to increase throughput and decrease the number of subjects resulting from human expertise in the detection of plant diseases [13].

The following two steps are added successively after the segmentation phase. The authors proposed and experimentally evaluated a software solution for automatic detection and classification of plant leaf diseases. Studies of plant trait/disease refer to the studies of visually observable patterns of a particular plant. Nowadays, crops face many traits/diseases. Insect damage is one of the major traits/diseases. Insecticides are not always proven efficient because they may be toxic to some form of bird and damage natural animal food chains. They determine the pixels that are primarily green in the first step. Next, these pixels are masked based on threshold amounts that are derived using Otsu's approach, then those primarily green pixels are masked. The second extra step involved removing all pixels on the edges of the infected cluster (object) and those with zeros for red, green, and blue values. The experimental findings show that the suggested method is a reliable way to identify illnesses in plant leaves. The effectiveness of the devised algorithm can successfully detect and classify the diseases under investigation with a precision of 83% to 94%, and it can achieve a 20% speedup over the research method [14].

A method for characterizing soybean seeds using image processing techniques has been reported by the authors [15]. Additionally, they have linked their model to immature soybean seeds, viral diseases, and fungal damage. For inspection and grading, a multivariate decision model based on Red, Green, and Blue (RGB) color features distinguished between asymptomatic and symptomatic seeds. The asymptomatic and symptomatic seeds had different colors, according to the color analysis. To describe the seed symptoms, a model was created that included six color variables, including averages, minimums, and variations for RGB pixel values. Some of the disparities among symptoms were not well described by color alone, according to the color analysis. With the highest chance of occurrence, a linear discriminant function with uneven priors for asymptomatic and symptomatic seeds produced an overall classification accuracy of 88%. The categorization accuracy for everyone was 97% asymptomatic, 30% Alternaria spp., 83% Cercospora spp., 62% Fusarium spp., 91% green immature seeds, 45% Phomopsis spp., 81% black soybean mosaic potyvirus, and 87% brown soybean mosaic potyvirus. The classifier's performance was unaffected by the seed's sampling year. The work was effective in creating a color-based knowledge domain and a color classifier enabling the creation of intelligent automated grain grading systems in the future.

Plant diseases result in significant output and financial losses for the global agriculture sector. For sustainable agriculture, it is essential to track the health of plants and trees and identify any diseases. As far as we are aware, there isn't a commercially available sensor that can measure the health of trees in real time. The most popular method for tracking tree stress now is scouting, which is costly, time-consuming, and labor-intensive. Plant diseases that necessitate a thorough sampling and processing method are identified using molecular techniques like polymerase chain reaction. Productivity can be increased by using early information on crop health and disease detection to help control diseases through appropriate management techniques such as vector control with pesticide, fungicide, and disease-specific chemical applications.

The necessity for a quick, affordable, and accurate health-monitoring sensor that would support agricultural improvements is acknowledged in this research. It outlines the technologies now in use that can be applied to the development of a ground-based sensor system that could assist in identifying plant diseases and health in field settings. These technologies include approaches for detecting plant diseases that are based on imaging and spectroscopy as well as volatile profiling. The advantages and disadvantages of various possible approaches are contrasted in the paper [5].

This work presents an algorithm that uses color and texture information to categorize five different types of rice. Image acquisition, segmentation, feature extraction, feature selection, and classification are the phases that make up the suggested approach. From rice kernels, 60 color and texture characteristics were recovered. Four distinct methods were used to analyze the characteristics because the set comprised redundant, noisy, or even useless information. Twenty-two features were ultimately chosen as the best. To categorize rice types, a classifier based on back propagation neural networks was created. A total classification accuracy of 96.67% was attained [16].

The automation or semi-automation of the seed quality purity test is reviewed in this work. Although computer vision (CV) technology is a sophisticated form of inspection technology utilized in many other industries, its application in agriculture is very limited. Using CV technologies in agriculture is quite difficult. Research in this field has been prompted by the significance of CV in this field. There is a brief discussion of several theories on the automation of seed quality purity tests. Features and classifiers are used to categorize the reviewed methods. The article discusses the techniques for identifying a specific seed's characteristics as well as the classifiers that were employed to categorize the seeds. A summary of the most widely used techniques for seed feature extraction and categorization is provided. Regardless of the specific feature or classifier, the paper's main objective is to give academics working on automated seed categorization a comprehensive reference source [17].

In this study, anthracnose-affected lesion areas are divided using segmentation techniques, graded according to the proportion of affected area, and classified as normal and anthracnose-affected fruits using a neural network classifier. For our study, we have taken into consideration three different kinds of fruit: pomegranates, grapes, and mangos. There are two stages to the established processing scheme. In the first stage, lesion areas afflicted by anthracnose are separated from normal areas using segmentation techniques such as thresholding, region expanding, K-means clustering, and watershed. The percentage of affected areas is then used to grade these affected locations. The run-length matrix is used in the second step to extract texture features. After that, an ANN classifier is employed to classify these features. We experimented using a collection of 600 picture samples of fruits. Normal and afflicted anthracnose fruit varieties have classification accuracy of 84.65% and 76.6%, respectively. The study is used in the horticulture industry to construct a machine vision system [18].

3 Proposed Methodology

This chapter covers the suggested method's pre-processing, algorithm, and flow chart. The proposed method of normal and disease-affected crops has been applied on corn seeds, which have been collected from the Agriculture Department, Bahawalpur. The results and their discussions are depicted in Chapter 4.

3.1 Methodology

In this research work, several steps have been executed to create a system capable of discriminating against and classifying normal and diseased corn seeds. The developed system used machine vision and artificial intelligence techniques. Further, image acquisition, preprocessing for enhancement of corn seed images, edge detection of corn seed images, sharpening of corn seed images, some morphological operations on corn seed images, suitable features selection and extraction of images and application of a suitable classifier have been outlined in this section. The details of each phase are as below. Figure 2 represents the steps of the suggested system executed to develop the system.

Start: Convert the dataset into JPEG format	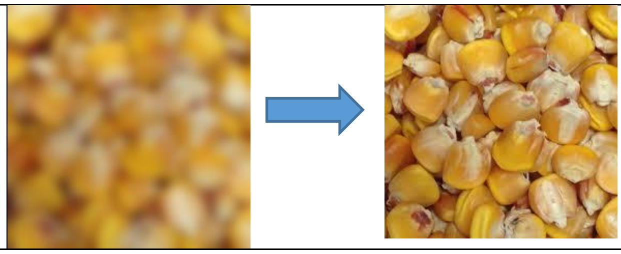

Pre-processing:
Local Histogram Equalization

Feature Extraction:
Each of the four orientations (π, π/2, π/3, and π/4) has a Gabor texture descriptor. The co-occurrence matrix is applied to each local histogram equalized image and the four images that are derived from the Gabor texture descriptor.

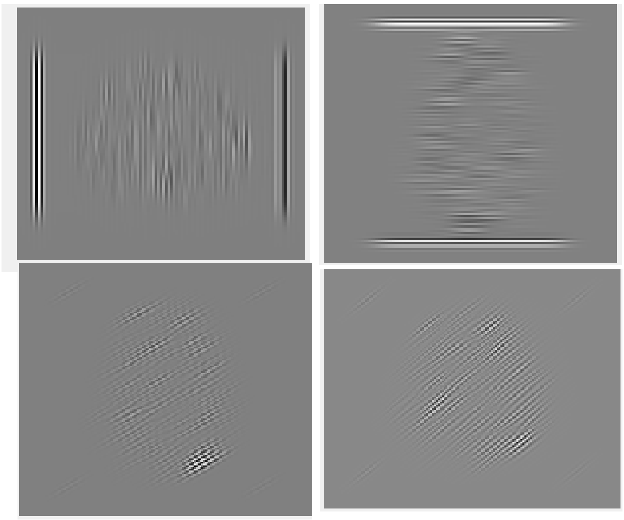

Combining features:
Combining extracted features

smoth_0	kurt_0	entrp_0	contrast2_	mean_0
0.999841	2.945997	4.830552	1125.106	198.3311
0.999744	7.450287	2.593456	462.4325	228.4244
0.999838	2.996088	4.688709	863.1534	200.4996
0.999844	2.726321	4.833203	886.843	196.5822
0.999835	2.88819	4.816932	1003.007	198.7402
0.999835	2.801735	4.998729	942.9221	197.0162
0.999837	2.737084	5.044137	1106.191	196.3825
0.999837	2.698331	5.118662	1055.592	195.526
0.999839	2.73567	5.062974	1139.763	195.6375
0.999845	2.688558	5.002384	1133.336	195.0343
0.999838	2.847195	4.854786	1175.991	197.7044
0.999837	2.977203	4.832567	1009.249	198.8864
0.999839	2.786293	4.900312	1097.415	196.8231
0.999836	2.897249	4.904982	1093.629	197.8292

Classification using SVM:

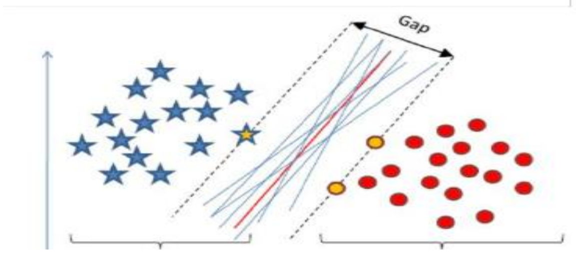

Figure 2. Top-down approach of the proposed system

3.2 Image acquisition

A newly created and tailored dataset for research and experiments was gathered from the Agriculture Department in Bahawalpur. The dataset was obtained using a digital camera with large dimensions, high megapixels, and no compression ratio. The photos utilized for each seed's study and experiments are detailed in Table 1. A total of 1800 photos from various seed classes—600 photos from each seed category—have been used for studies and tests. Of these 1800 photos, 1188 (396 of each seed category) were used to train the suggested approach, and 612

(204 of each seed category) were utilized to test the published method [8].

Table 1. Number of photos utilized to test and train the suggested technique

Seed Type	Total number of images	No. of Images used for Training	No. of Images used for Testing
Cotton	600	396	204
Wheat	600	396	204
Corn	600	396	204
Total	**1800**	**1188**	**612**

3.3 Preprocessing

An image has undergone many operations at this step. To utilize the surface data for inclusion extraction and order, the dataset's photos were first converted to JPEG, which is an acceptable picture format. Despite this, the digital camera utilized to gather datasets provided very high-quality and determined outputs.

3.4 Feature representation

Feature extraction is to find representation of the textural data relating to pixel and tissue relationship. That is the reason, the primary concern of the study was to select a more appropriate set of features for the dataset. The set of features selected were on the criteria that they must have maximum textural information in connection with their spatial and neighboring relationship [19]. In this way, it can be a superior decision among texture descriptors for the investigation of agriculture related information, i.e., normal (healthy) or abnormal (diseased) seeds. Figure 3 shows the Gabor filtered slices with four orientations (π, $\pi/2$, $\pi/3$ and $\pi/4$). The 2D Gabor filter is mathematically described in Eq. 2 and Eq. 3.

$$g\lambda, \theta, \phi, \sigma, \gamma\,(x, y) = \exp\left(-\frac{x' + \gamma 2y'}{2\sigma^2}\right)\cos\left(2\pi\frac{x'}{\lambda} + \phi\right) \quad (2)$$

$$x' = x\cos\theta + y\sin\theta,\; y' = y\cos\theta - x\sin\theta \quad (3)$$

The results of Gabor filter (for all four angles of π, $\pi/2$, $\pi/3$ and $\pi/4$) applied on each sample image of cotton, wheat and corn seed has been shown in Figure 3.

Seed Type	Cotton Image	Wheat Image	Corn Image
Original Image			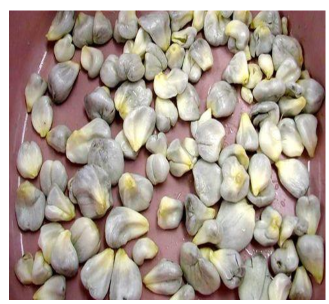
	(a)	(f)	(k)

Resultant image when Gabor filter at angle π has been applied	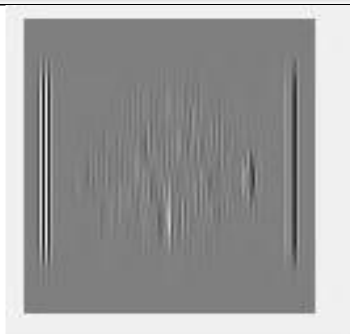	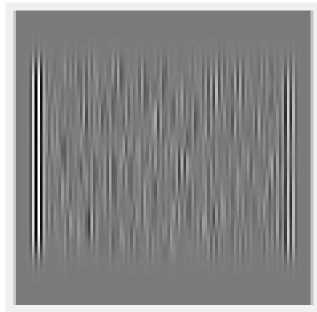	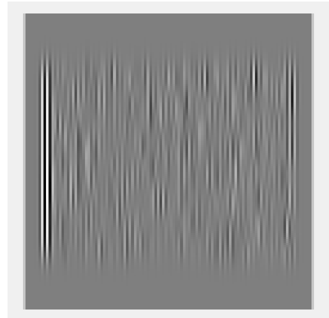
	(b)	(g)	(l)
Resultant image when Gabor filter at angle π/2 has been applied		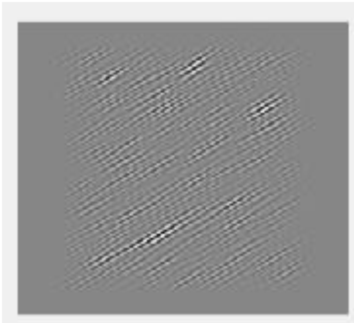	
	(c)	(h)	(m)
Resultant image when Gabor filter at angle π/3 has been applied			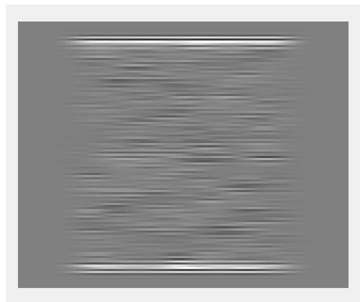
	(d)	(i)	(n)
Resultant image when Gabor filter at angle π/4 has been applied	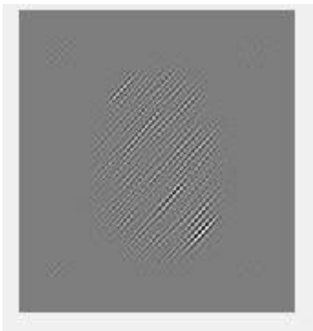	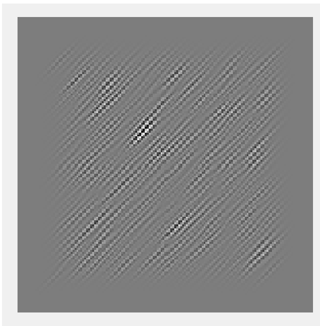	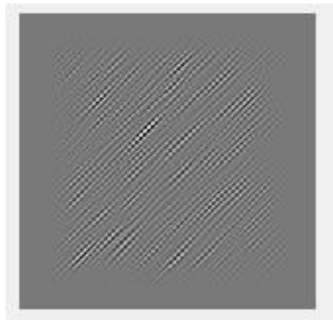
	(e)	(j)	(o)

Figure 3. Showing original images of cotton, wheat and corn seeds and their Gabor features on four angles π, π/2, π/3 and π/4 (a) original image of abnormal cotton seeds (b) resultant image of (a) when Gabor texture filter has been applied on angle π (c) resultant image of (a) when Gabor texture filter has been applied on angle π/2 (d) resultant image of (a) when Gabor texture filter has been applied on angle π/3 (e) resultant image of (a) when Gabor texture filter has been applied on angle π/4 (f) original image of abnormal wheat seeds (g) resultant image of (f) when Gabor texture filter has been applied on angle π (h) resultant image of (f) when Gabor texture filter has been applied on angle π/2 (i) resultant image of (f) when Gabor texture filter has been applied on angle π/3 (j) resultant image of (f) when Gabor texture filter has been applied on angle π/4 (k) original image of corn abnormal seeds (l) resultant image of (k) when Gabor texture filter has been applied on angle π (m) resultant image of (k) when Gabor texture filter has been applied on angle π/2 (n) resultant image of (k) when Gabor texture filter has been applied on angle π/3 (o) resultant image of (k) when Gabor texture filter has been applied on angle π/4

In the resulting GLCM, each component (i, j) is essentially the sum of the conditions under which a pixel with value i occurred in the predetermined spatial relationship to a pixel with value j in the input image [20].

3.5 Feature extraction

By predicting specific qualities, or highlights, that distinguish one information design from another example, feature extraction aims to reduce the initial information. By considering the representation of the relevant aspects of the image into feature vectors, the extracted highlight should provide the classifier with the attributes of the information composed [19]. The texture features listed below have been extracted:

- **Contrast:** The intensity contrast between a pixel and its neighbor throughout the entire image is measured by the contrast function. A contrast range of [0 (size (GLCM, 1)-1)^2] is available. A continuous image has no contrast. The formula below is used to calculate contrast:

$$C = \sum_{i,j} |i-j|^2 P(i,j)$$

- **Homogeneity:** A value indicating how closely the distribution of GLCM elements adheres to the GLCM diagonal is returned by homogeneity. [0 1] is the range of homogeneity. When a GLCM is diagonal, homogeneity is 1. The following equation is used to assess homogeneity:

$$H = \sum_{i,j} \frac{P(i,j)}{1+|i-j|}$$

- **Mean:** The value in the image where central clustering takes place is estimated by the mean, m, of the pixel values inside the specified frame. The following formula can be used to get the mean:

$$\mu = \frac{1}{MN}\sum_{i=1}^{M}\sum_{j=1}^{N} p(i,j)$$

Where p (i, j) is the pixel value at point (i, j) of an image of size M x N.

- **Kurtosis:** K measures the peakedness or flatness of a distribution relative to a normal distribution. The conventional definition of kurtosis is:

$$K = \left\{\frac{1}{MN}\sum_{i=1}^{M}\sum_{j=1}^{N}\left[\frac{p(i,j)-\mu^4}{\sigma}\right]\right\} - 3$$

Where, p (i, j) is the pixel value at point (i, j), m and σ are the mean and standard deviation, respectively. The -3 term makes the value zero for a normal distribution.

- **Smoothness:** Descriptors of relative smoothness can be established using relative smoothness, or R, a measure of grey level contrast. The following formula determines the smoothness: $$R = 1 - \frac{1}{1+\sigma^2}$$
- **Entropy:** The texture of the input image can be described using entropy, a statistical measure of randomness. The distribution variation in a region can also be described by entropy, h. The image's overall entropy can be computed as follows:

$$h = -\sum_{K=0}^{L-1} Pr_k(log_2 Pr_k)$$

Where Pr is the probability of the k-th grey level, which can be calculated as Zk /m*n, Zk is the total number of pixels with the k-th grey level and L is the total number of grey levels.

3.6 Classifiers

In this proposed study, several classifiers have been used to compare classification rates. It was desired to achieve maximum classification rates. For this, following classifiers were experimented with: Support Vector Machine (SVM), K-Nearest Neighbours (KNN), multiclass classifier, Artificial Neural Networks (ANNs), trees, regression models and ensembles. The classifier, which achieved maximum classification rates, has been used to build the learned model, which is used by providing an interface for the classification of new data (seed image in this case). Every classifier was trained and validated using five-fold cross-validation on the 1,188-image training partition, and the rates reported in Section 4 are averaged over five folds; the held-out 612 images were used only for final testing.

3.7 Evaluation measures

Any implemented methodology's performance and efficacy are evaluated using evaluation measures. Below is a detailed list of the standard evaluation metrics that were utilized to assess the suggested approach.

Accuracy= $\frac{TP+TN}{TP+TN+FP+FN}$

Sensitivity= $\frac{TP}{TP+FN}$

Specificity= $\frac{TN}{TN+FP}$

FNR= $\frac{FN}{TP+FN}$

Precision= $\frac{TP}{TP+FP}$

FPR= $\frac{FP}{FP+TN}$ or 1- accuracy

4 Results and Discussions

The methodology used by the proposed system was described in detail in section 3, which also included a discussion of the pre-processing, algorithm, and flow chart of the proposed method. The results of the proposed methodology were presented in this chapter along with a discussion of them.

4.1 Experimental results

Most agricultural studies are motivated by the creation of applications to extract distinctive information from photographs belonging to different classes. The photos utilized for research and tests with each seed class are detailed in Table 1. Research and trials have been conducted using a total of 1800 photos, 600 of which are from each of the seed categories. The suggested approach was trained using 1188 (396 photos of each category of seeds class) of these 1800 images and the reported method was tested using 612 (204 images of each category seed class).

Results regarding the normal (healthy) and diseased (abnormal) classification of several seeds have been obtained in this experiment using Gabor texture characteristics that have been post-applied using a co-occurrence matrix on each feature. Each method's results are averaged across five times in the datasets, and rates are expressed as percentages (i.e., the ratio of right decisions to total decisions). Furthermore, these techniques are tested on 1188 photos, which include pictures depicting different expressions and captured in a range of lighting conditions. Every image in each dataset had its texture, shape, and color features extracted before being concatenated into a single feature vector. Table 2 shows a sample of these textural characteristics for both healthy and diseased cotton seeds, and Annexure C in the thesis report contains a comprehensive list of all the characteristics, where texture features are represented by the letters F1, F2, F3, F4, F5, F6, and F7.

Table 2. Sample representation of texture features for both normal and diseased seed of cotton

F1	F2	F3	F4	F5	F7	Class
0.00926	0.0962	1124.2097	1265280.602	2030.487222	3.566E-11	**Normal**
0.01306	0.1142	1123.2078	1262223.966	2490.22007	2.313E-11	**Diseased**
0.01590	0.1261	1135.5084	1298940.37	2805.291531	2.067E-11	**Normal**
0.01082	0.1040	1123.6202	1263447.882	2232.725984	3.031E-11	**Diseased**
0.01045	0.1022	1122.5842	1260354.787	2182.687145	2.949E-11	**Normal**
0.01064	0.1032	1123.7752	1263923.273	2209.684083	3.007E-11	**Diseased**

On similar pattern a sample of these texture features for both corn normal and diseased seeds is represented in Table 3, while a complete list of features has been presented in the thesis report as an Annexure D.

Table 3. Sample representation of texture features for both normal and diseased seed of corn

F1	F2	F3	F4	F5	F7	Class
0.00021	0.5517	0.736935	26.92981379	2.844432698	35.26263	**Normal**
0.00022	0.5552	0.746242	24.38471734	2.840743467	39.08153	**Diseased**
0.00020	0.5473	0.742142	25.25084757	2.878886102	37.35577	**Normal**
0.00020	0.5435	0.736024	26.06237688	2.907127738	36.97094	**Diseased**
0.00020	0.5369	0.760067	21.41891974	2.827466131	40.42363	**Normal**
0.00021	0.5694	0.744931	25.2685024	2.767769768	36.74299	**Diseased**

Similarly, a sample of these texture features for both wheat normal and diseased seeds is represented in Table 4, while a complete list of features has been presented in the thesis report as an Annexure E.

Table 4. Sample representation of texture features for both normal and diseased seed of wheat

F1	F2	F3	F4	F5	F7	Class
27.8343	0.3259	3.9127331	0.636822801	0.622269243	0.569864	**Normal**
22.9334	0.3784	3.5748751	0.673143406	0.659096743	0.614864	**Diseased**
28.3948	0.2913	4.1865236	0.60847221	0.592198358	0.538601	**Normal**
30.4924	0.2879	4.1755663	0.607308901	0.591657673	0.535130	**Diseased**
29.1543	0.3208	3.9322217	0.633590587	0.61963977	0.565193	**Normal**
26.9651	0.3097	4.0950780	0.62102287	0.604993703	0.555717	**Diseased**

In order to evaluate the effectiveness and performance of the proposed method, numerous experiments have been conducted on various seed class images. The standard evaluation measures, such as accuracy, specificity, sensitivity, and ROC curve values, have been used in the experiments because most related studies have also used these standard quantitative parameters for the evaluation of their proposed methods.

- True Positive (TP): correctly identified.
- False Positive (FP): incorrectly identified.
- True Negative (TN): correctly rejected.
- False Negative (FN): incorrectly rejected.

The studies were conducted using several classifiers on both the Weka 3.8.1 and MATLAB 2016b tools. The following is a list of the quantitative parameters used to assess the suggested approach using MATLAB and Weka:

- Sensitivity or True Positive Rate (TPR) = TP / (TP + FN). (eqv. with recall)

- False Positive Rate (FPR) = FP / (FP + TN).
- False Negative Rate (FNR) = 1 – TPR.
- Precision or Positive Predictive Value (PPV) = TP / (TP + FP).
- False Discovery Rate (FDR) = 1 – PPV.
- F-Measure is the weighted harmonic mean of recall and precision.
- Receiver Operating Characteristic (ROC).
- Mean Absolute Error (MAE).
- Root Mean Square Error (RMSE).

Cotton seeds were classified as normal (healthy) or diseased (abnormal) using MATLAB. Table 5 shows the accuracy, true positive rate, false negative rate, positive predictive value, false discovery rate, and ROC-curve values.

Table 5. Results obtained through MATLAB for cotton seeds classification as normal (healthy) and diseased (abnormal)

Sr#	Classifier	Accuracy	TPR	FNR	PPV	FDR	ROC value
1	Ensemble (RUS Boosted Trees)	**83.8%**	86%	14%	89%	11%	0.90
2	SVM (Cubic SVM)	83.2%	88%	12%	87%	13%	0.86
3	Linear Discriminant	83.5%	91%	9%	85%	15%	0.86

The findings obtained using MATLAB on cotton seeds for the classification of seeds as normal and diseased are displayed in Table 5. Training and testing have been conducted on 600 photos in total. The suggested approach was trained using 396 of these 600 photos, and the suggested scheme was tested using 204 of them. In contrast to SVM and linear discriminant classifiers, which have accuracy measures of 83.2% and 83.5%, respectively, this ensemble classifier achieves the highest accuracy of 83.8%, as shown in Table 5. As we can see from Table 5, the Ensemble classifier produced TPR and PPV values of 86% and 89%, respectively. The same information represented as a graph has been depicted in Figure 4.

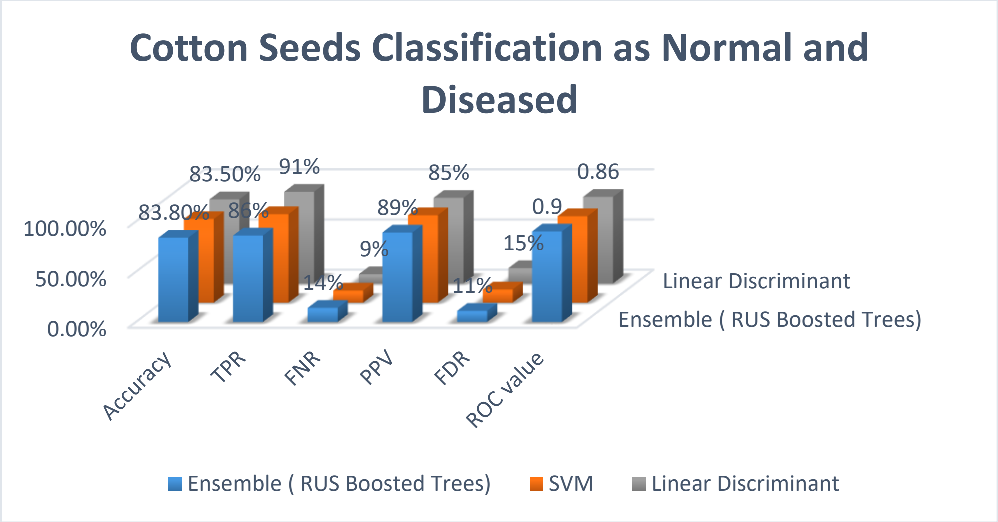

Figure 4. Comparisons of different classifiers on cotton seeds for the classification of normal seeds and abnormal (diseased) seeds as per standard evaluation measures, i.e., accuracy, specificity, sensitivity and ROC value (AUC curve)

Spectrum of Engineering Sciences
ISSN (e) 3007-3138 (p) 3007-312X Volume 4, Issue 3, 2026

Table 6 shows the classification results for cotton seeds as normal (healthy) and diseased (abnormal) using the Weka machine learning technology. Accuracy, true positive rate, false negative rate, positive predictive value, false discovery rate, and ROC-curve values are also shown.

Table 6. Results obtained through Weka for the classification of cotton seeds as normal and abnormal (diseased)

Classifier Used for Classification	TP-Rate	FP-Rate	Precision	Recall	F-Measure	ROC(AUC)	Mean Absolute Error	Root Mean Square	Class
Multilayer Perceptron 71.9794%	0.672	0.227	0.765	0.672	0.715	0.754	0.2958	0.479	Normal
	0.773	0.328	0.681	0.773	0.724	0.754			Diseased
	0.72	0.275	0.725	0.72	0.72	0.754			Weighted Avg.
Rules (JRip) 74.036	0.681	0.206	0.75	0.681	0.714	0.759	0.3436	0.4493	Normal
	0.794	0.319	0.733	0.794	0.762	0.759			Diseased
	0.74	0.265	0.741	0.74	0.739	0.759			Weighted Avg.
Rules (PART) 71.9794%	0.773	0.328	0.681	0.773	0.724	0.754	0.2958	0.479	Normal
	0.672	0.227	0.765	0.672	0.715	0.754			Diseased
	0.72	0.275	0.725	0.72	0.72	0.754			Weighted Avg.
Trees (Random Tree) 78.4062%	0.741	0.176	0.792	0.741	0.765	0.782	0.2159	0.4647	Normal
	0.824	0.259	0.778	0.824	0.8	0.782			Diseased
	0.784	0.22	0.784	0.784	0.784	0.782			Weighted Avg.

At the same time, both MATLAB and Weka were used to construct a trained model for the classification of wheat seeds for its normal and abnormal class categorization. Accuracy, TP-Rate, FP-Rate, TN-Rate, FN-Rate, F-measure, Precision, Recall, ROC (AUC) Value, Mean Absolute Error, and Mean Square Error are the typical assessment metrics that have been used to validate the results. These studies were conducted solely to validate and authenticate the findings for cross-validation purposes. Table 7 shows the accuracy, true positive rate, false negative rate, positive predictive value, false discovery rate, and ROC-curve of the classification findings for wheat seeds that were made using MATLAB as normal (healthy) and diseased (abnormal).

Table 7. Results obtained through MATLAB for the classification of normal and diseased seeds of wheat

Sr #	Classifier	Accuracy	TPR	FNR	PPV	FDR	ROC value
1	SVM (Cubic Kernel)	100%	100%	0%	100%	0%	1.00
2	Ensemble (Subspace KNN)	100%	100%	0%	100%	0%	1.00
3	SVM (Quadratic Kernel)	100%	100%	0%	100%	0%	1.00
4	SVM (Fine Gaussian Kernel)	100%	100%	0%	100%	0%	1.00

The findings of classifying wheat into normal and pathological classes are displayed in Table 8. Accuracy, TP-Rate, FP-Rate, TN-Rate, FN-Rate, F-measure, Precision, Recall, ROC (AUC) Value, Mean Absolute Error, and Mean Square Error are the typical assessment metrics that have been used to validate the results. These studies were conducted solely to validate and authenticate the findings for cross-validation purposes. The graph that represents the same data is shown in Figure 5.

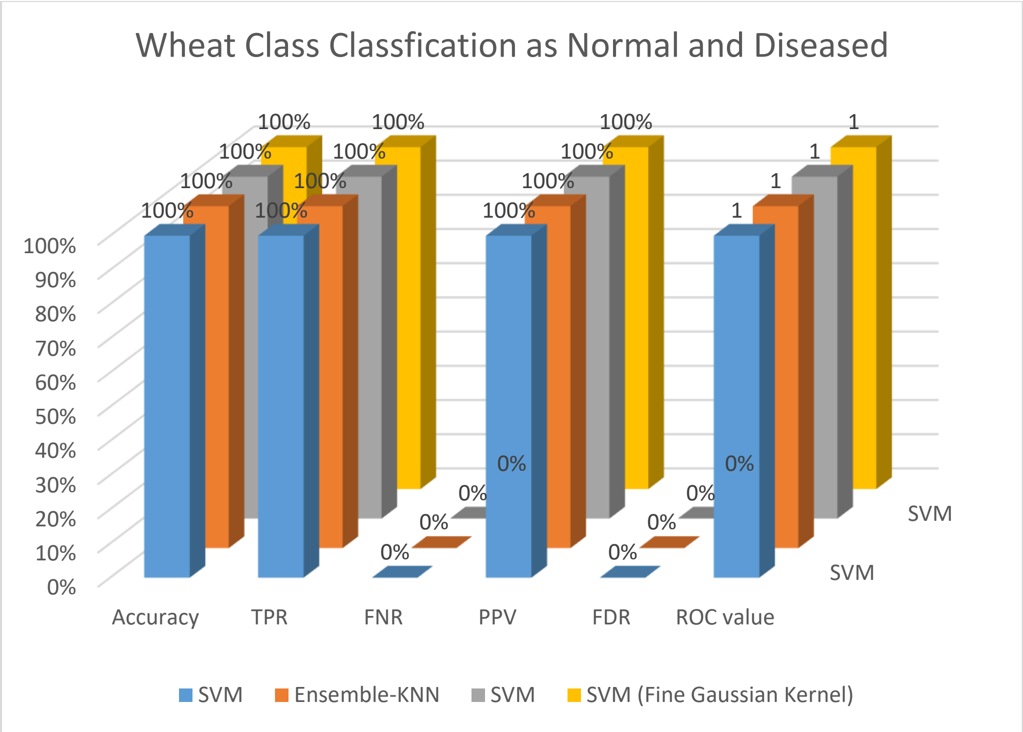

Figure 5. Comparisons of different classifiers on wheat seeds for the classification of normal seeds and abnormal (diseased) seeds as per standard evaluation measures, i.e., accuracy, specificity, sensitivity and ROC value (AUC curve)

Table 8. Results obtained through Weka for the classification of wheat seeds as normal and abnormal

Classifier Used for Classification	TP-Rate	FP-Rate	Precision	Recall	F-Measure	ROC(AUC)	Mean Absolute Error	Root Mean Square Error	Class
Misc (VFI) 80.83%	0.531	0	1	0.531	0.693	0.924	0.3868	0.4027	Normal
	1	0.469	0.755	1	0.861	0.924			Diseased
	0.808	0.278	0.855	0.808	0.792	0.924			Weighted Avg.
Lazy (IBK) 100%	1	0	1	1	1	1	0.0002	0.0002	Normal
	1	0	1	1	1	1			Diseased
	1	0	1	1	1	1			Weighted Avg.
Meta (Adaboost M1) 98%	0.951	0	1	0.951	0.975	1	0.0381	0.111	Normal
	1	0.049	0.967	1	0.983	1			Diseased
	0.98	0.029	0.981	0.98	0.98	1			Weighted Avg.
Meta (Bagging) 86.5%	1	0	1	1	1	1	0.0091	0.0473	Normal
	1	0	1	1	1	1			Diseased
	1	0	1	1	1	1			Weighted Avg.

Following the same pattern as the suggested approach, both MATLAB and Weka were utilized when a trained model was created for the classification of maize seeds into normal and abnormal classes. Accuracy, TP-Rate, FP-Rate, TN-Rate, FN-Rate, F-measure, Precision, Recall, ROC (AUC) Value, Mean Absolute Error, and Mean Square Error are the typical assessment metrics that have been used to validate the results. These studies were conducted solely to validate and authenticate the findings for cross-validation purposes. Table 9 shows the accuracy, true positive rate, false negative rate, positive predictive value, false discovery rate, and ROC-curve of the classification results derived from MATLAB for maize seeds as normal (healthy) and diseased (abnormal).

Table 9. Results obtained using MATLAB for the classification of normal and diseased corn seeds

Sr #	Classifier	Accuracy	TPR	FNR	PPV	FDR	ROC value
1	Ensemble(Subspace Discriminant)	**84.0%**	91%	9%	86%	14%	0.88
2	SVM (Cubic Kernel)	83.5%	89%	11%	87%	13%	0.87
3	SVM (Quadratic Kernel)	83.0%	90%	10%	85%	15%	0.89

The findings of the Weka machine learning tool's classification of corn into normal and pathological classes are displayed in Table 10. Accuracy, TP-Rate, FP-Rate, TN-Rate, FN-Rate, F-measure, Precision, Recall, ROC (AUC) Value, Mean Absolute Error, and Mean Square Error are the typical assessment metrics that have been used to validate the results. These studies were conducted solely to validate and authenticate the findings for cross-validation purposes. The graph that represents the same data is shown in Figure 6.

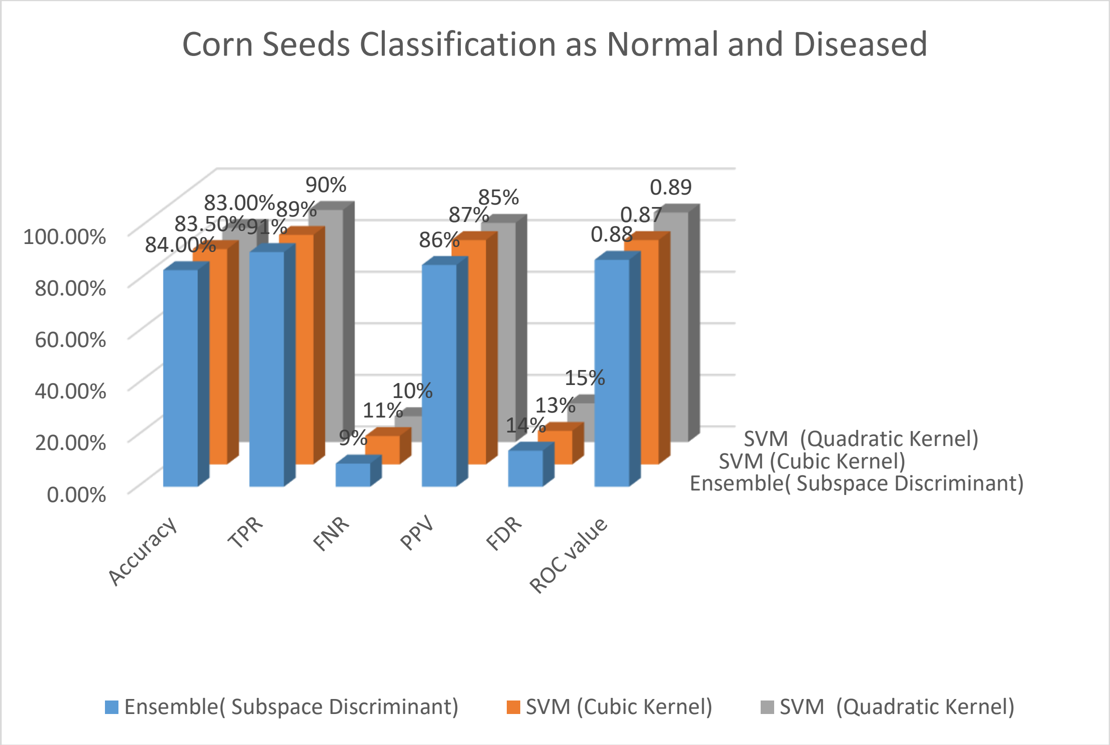

Figure 6. Comparisons of different classifiers on corn seeds for the classification of normal seeds and abnormal (diseased) seeds as per standard evaluation measures, i.e., accuracy, specificity, sensitivity and ROC value (AUC curve)

Table 10. Weka results for the classification of corn seeds as normal and diseased

Classifier Used for Classification	TP-Rate	FP-Rate	Precision	Recall	F-Measure	ROC(AUC)	Mean Absolute Error	Root Mean Square Error	Class
Trees (Simple cart) 78.1667%	0.858	0.374	0.823	0.858	0.84	0.769	0.274 1	0.4241	Normal
	0.626	0.142	0.685	0.626	0.654	0.769			Diseased
	0.782	0.297	0.778	0.782	0.779	0.769			Weighted Avg.
Function (SMO) 80.3333	0.933	0.46	0.805	0.933	0.864	0.737	0.196 7	0.4435	Normal
	0.54	0.067	0.799	0.54	0.645	0.737			Diseased

	0.803	0.33	0.803	0.803	0.792	0.737			Weighted Avg.
Functions (RBFNetwork) 78.3333%	0.866	0.384	0.821	0.866	0.843	0.769	0.324	0.4054	Normal
	0.616	0.134	0.693	0.616	0.652	0.769			Diseased
	0.783	0.302	0.779	0.783	0.78	0.769			Weighted Avg.
Bayes (bayesNet) 71.3333	0.746	0.354	0.811	0.746	0.777	0.801	0.287	0.5284	Normal
	0.646	0.254	0.557	0.646	0.598	0.799			Diseased
	0.713	0.321	0.727	0.713	0.718	0.8			Weighted Avg.

The results obtained for the corn class of seeds are displayed in Table 10. Training and testing have been conducted on 600 photos in total. Of these 600 photos, 396 were used to train the suggested approach, and 204 were utilized to test the suggested system. In contrast to the Simple CART and RBFNetwork classifiers, which achieved accuracy measures of 78.17% and 78.33%, respectively, the highest accuracy of 80.33% was produced by the SMO function classifier, as shown in Table 10. As we can see from Table 10, the SMO classifier produced weighted-average TP-rate and precision values of 0.803 each.

4.2 Comparison with state-of-the-art methods

Table 11 shows the results for cotton, wheat and corn seeds classification proposed by the researchers working in the domain of seeds classification and discrimination. The results obtained with the reported method have been compared with the previously published techniques. It is evident from Table 11 that the results obtained by the proposed method are significantly better than all the previously published methods.

Table 11. Comparison with the reported approach and the state-of-the-art methods of seeds classification

Method reported by/year	Methodology adopted	Classification of	Classification rates achieved
Shatadal, P and Tan, J, 2003	Color features in the RGB (red, green, blue) color space and Neural Network	Soybean Seeds Classification	99.6%
Kurtulmuş, F and Ünal, H, 2015 [90]	Computer vision and machine learning	Rapeseeds Classification into its seven varieties	99.24%
Wang, Haopeng and Li, Hui, 2015 [21]	Local binary pattern algorithm (LBP), and gray level co-occurrence matrix algorithm (GLCM) (LBP-GLCM)	Classification and recognition of impurities in cotton seeds	Dead cotton (90%) and Barren cotton (88%)
The Proposed Method	**Texture Parameters+ Gabor Filter+ Co-Occurrence Matrix + SVM + Ensembles classifiers**	Cotton seeds	**83.8%**
		Wheat seeds	**100%**
		Corn Seeds	**84.0%**

As we observed from the Table 11, the method reported by Shatadal, P and Tan, J only classified soybean seeds. They have calculated color features from RGB encoding scheme based images. Each color component, i.e., red, green and blue has been used for their color features, then artificial neural network has been employed for machine learning. Resultantly, the accuracy achieved on soybean seeds remained 99.6%, which is appreciable. However, ANN based learned model always remained computationally complex. Further, they have only trained their model to classify only soybean seeds.

Another approach reported by Kurtulmuş, F and Ünal, H classified rapeseeds into their seven varieties. They also used computer vision and machine learning models for the classification of their results. Their reported approach achieved accuracy for rapeseed as 99.24%, which is also appreciable. In another approach, investigated by Wang, Haopeng and Li, Hui for the classification of cotton seeds has been published in the literature. They used local binary patterns and gray level co-occurrence matrix for feature representation and features extraction. With their approach, the results remained 90% and 88% for dead cotton seeds and barren cotton seeds, respectively.

In the reported approach, we have used the power of Gabor texture filters along with co-occurrence matrix and other texture parameters. After having features set extracted through these techniques, different machine learning models have been experimented so that a model could be trained in an optimal manner, which is able to deal with the classification of cotton, wheat and corn seeds as normal (healthy) and abnormal (diseased) ones. Using the proposed approach, the standard evaluation measures in terms of accuracy for cotton, wheat and corn remained 83.8%, 100% and 84.0% respectively. The proposed approach is more efficient in terms of its computational complexity because it does not need complex training on each new instance.

4.3 Limitations

Three limitations of this study should be noted. First, the 100% accuracy reported for wheat across all four MATLAB classifiers (Table 7), and for two of the Weka classifiers (Table 8), is unlikely to generalize. Values of this kind usually indicate that the normal and diseased wheat images are separable on an incidental cue — acquisition session, background, or illumination — rather than on seed texture alone. Because all images of a given crop were captured under a single acquisition protocol, an image-level split cannot rule out leakage between correlated images of the same seed lot. A seed-lot-level (grouped) split, and an independently acquired test set are therefore required before the wheat result can be accepted at face value. Second, the dataset is modest — 600 images per crop — and was collected from a single source, the Agriculture Department, Bahawalpur, so performance on seeds from other regions, cultivars, and imaging devices remains unknown. Third, the reported figures are point estimates from a single cross-validation run; no confidence intervals or repeated-run variances are given, so differences of less than one percentage point between the leading classifiers in Tables 5 and 9 should not be treated as meaningful.

5 Conclusion

The development of automated methods for classification has been made possible by the maturation of computer vision and machine learning models. The simplicity of computation and the decrease in operator involvement are the foundations of these methods' applicability in various real-world units. As a result, the Department of Agriculture is currently receiving assistance from machine learning, computer vision, and other relevant fields. Using these multidisciplinary approaches, a plan was put forth in this analysis to handle both healthy and infected seeds for each of the three categories—corn, wheat, and cotton. The disclosed approach has employed the Gabor filter for feature extraction and local histogram equalization as a pre-processing step. The learned model was trained using an SVM with a cubic kernel. A significant number of experiments were conducted on the three seed datasets to assess the robustness of the approach, its ability to detect deviation from the norm, and its overall classification performance.

References

Arribas, J.I., et al., *Leaf classification in sunflower crops by computer vision and neural networks.* Computers and Electronics in Agriculture, 2011. **78**(1): p. 9-18.

Lee, W., et al., *Sensing technologies for precision specialty crop production.* Computers and electronics in agriculture, 2010. **74**(1): p. 2-33.

Sankaran, S., et al., *A review of advanced techniques for detecting plant diseases.* Computers and Electronics in Agriculture, 2010. **72**(1): p. 1-13.

Kuz, A., M. Falco, and R. Giandini, *Análisis de redes sociales: un caso práctico.* Computación y sistemas, 2016. **20**(1): p. 89-106.

Mendoza, L.E., M.A. Pérez, and A.C. Grimán, *Prototipo de modelo sistémico de calidad (MOSCA) del software.* Computación y sistemas, 2005. **8**(3): p. 196-217.

Serna, E., R. Martínez, and P. Tamayo, *Una revisión a la realidad de la automatización de las pruebas del software.* Computación y Sistemas, 2019. **23**(1): p. 169-183.

Yáñez Márquez, C. and J.L. Díaz de León Santiago, *Memorias asociativas basadas en relaciones de orden y operaciones binarias.* Computación y Sistemas, 2003. **6**(4): p. 300-311.

Argiculture Department, B., *Seeds Dataset*, B. Argiculture Department, Editor. 2018.

Khera, E.A., et al., *Characterization of Nickel Oxide Thin Films for Smart Window Energy Conversion Applications: Comprehensive Experimental and Computational Study.* Available at SSRN 4235112.

Attique, M., et al., *Colorization and automated segmentation of human T2 MR brain images for characterization of soft tissues.* PloS one, 2012. **7**(3): p. e33616.

Ullah, H., et al., *M-mode swept source optical coherence tomography for quantification of salt concentration in blood: an in vitro study.* Laser Physics, 2012. **22**: p. 1002-1010.

Gilanie, G., *Spectroscopy of T2 weighted brain MR image for object extraction using prior anatomical knowledge based spectroscopic histogram analysis*. 2013.

Gilanie, G., et al., *Object extraction from T2 weighted brain MR image using histogram based gradient calculation.* Pattern Recognition Letters, 2013. **34**(12): p. 1356-1363.

Ullah, H., et al., *Autocorrelation optical coherence tomography for glucose quantification in blood.* Laser Physics Letters, 2015. **12**(12): p. 125602.

Asghar, K., et al., *Automatic Enhancement Of Digital Images Using Cubic BÃ© zier Curve And Fourier Transformation.* Malaysian Journal of Computer Science, 2017. **30**(4): p. 300-310.

Janjua, H.U., et al., *Classification of liver cirrhosis with statistical analysis of texture parameters.* International Journal of Optical Sciences, 2017. **3**(2): p. 18-25.

Bajwa, U.I., et al., *Computer-aided detection (CADe) system for detection of malignant lung nodules in CT slices-a key for early lung cancer detection.* Current Medical Imaging, 2018. **14**(3): p. 422-429.

Gilanie, G., et al., *Classification of normal and abnormal brain MRI slices using Gabor texture and support vector machines.* Signal, Image and Video Processing, 2018. **12**: p. 479-487.

Gilanie, G., et al., *Colored Representation of Brain Gray Scale MRI Images to potentially underscore the variability and sensitivity of images.* Current Medical Imaging Reviews, 2018. **14**(4): p. 555-560.

Janjua, H.U., A. Jahangir, and G. Gilanie, *Classification of chronic kidney diseases with statistical analysis of textural parameters: a data mining technique.* International Journal of Optical Sciences, 2018. **4**(1): p. 1-7.

Ullah, H., A. Batool, and G. Gilanie, *Classification of Brain Tumor with Statistical Analysis of Texture Parameter Using a Data Mining Technique.* International Journal of Industrial Biotechnology and Biomaterials, 2018. **4**(2): p. 22-36.

Gilanie, G., *Automated Detection and Classification of Brain Tumor from MRI Images using Machine Learning Methods.* 2019, Department of Computer Science, COMSATS University Islamabad, Lahore campus.

Gilanie, G., et al., *Automated and reliable brain radiology with texture analysis of magnetic resonance imaging and cross datasets validation.* International Journal of Imaging Systems and Technology, 2019. **29**(4): p. 531-538.

Gilanie, G., et al., *Computer aided diagnosis of brain abnormalities using texture analysis of MRI images.* International Journal of Imaging Systems and Technology, 2019. **29**(3): p. 260-271.

Amjad, M., et al., *Fourier-Transform Infrared Spectroscopy (FTIR) for Investigation of Human Carcinoma and Leukaemia.* Lasers in Engineering (Old City Publishing), 2021. **51**.

Gilanie, G., et al., *Risk-free WHO grading of astrocytoma using convolutional neural networks from MRI images.* Multimedia Tools and Applications, 2021. **80**(3): p. 4295-4306.

Gilanie, G., et al., *Coronavirus (COVID-19) detection from chest radiology images using convolutional neural networks.* Biomedical Signal Processing and Control, 2021. **66**: p. 102490.

Gilanie, G., et al., *RiceAgeNet: Age Estimation of Pakistani Grown Rice Seeds using Convolutional Neural Networks.* International Journal of Computational Intelligence in Control, 2021. **13**(2): p. 831-843.

Gilanie, G., et al., *RiceNet: convolutional neural networks-based model to classify Pakistani grown rice seed types.* Multimedia Systems, 2021: p. 1-9.

Gilanie, G., et al., *Digital Image Processing for Ultrasound Images: A Comprehensive.* Digital Image Processing, 2021. **15**(3).

Malik, S., et al., *Enhancing Contrast in Optical Imaging of Cancer tissues and Study the Spectral Properties of Methylene Blue.* Acta Microscópica, 2021. **30**(2): p. 49-57.

Rafiq, M., et al., *Reconstruction of scene using corneal reflection.* Multimedia Tools and Applications, 2021: p. 1-17.

Ghaffar, A.A., et al. *Refined Sentiment Analysis by Ensembling Technique of Stacking Classifier*. in *International Conference on Soft Computing and Data Mining*. 2022. Springer.

Gilanie, G., et al., *An Automated and Real-time Approach of Depression Detection from Facial Micro-expressions.* Computers, Materials & Continua, 2022. **73**(2).

Gilanie, G., et al. *FERNet: A Convolutional Neural Networks Based Robust Model to Recognize Human Facial Expressions*. in *International Conference on Soft Computing and Data Mining*. 2022. Springer.

Iqbal, M.J., et al., *Automatic brain tumor segmentation from magnetic resonance images using superpixel-based approach.* Multimedia Tools And Applications, 2022. **81**(27): p. 38409-38427.

Rubab, S.F., et al. *The Comparative Performance of Machine Learning Models for COVID-19 Sentiment Analysis*. in *International Conference on Soft Computing and Data Mining*. 2022. Springer.

Ullah, H., et al., *Diagnosis of Ocular Diseases Using Optical Coherence Tomography (OCT) at λ= 840 nm.* Lasers in Engineering (Old City Publishing), 2022. **53**.

Wazir, E., et al. *Early Stage Detection of Cardiac Related Diseases by Using Artificial Neural Network*. in *International Conference on Soft Computing and Data Mining*. 2022. Springer.

Yaseen, M., et al., *In-vitro Evaluation of Anticancer Activity of Rhodamine-640 perchlorate on Rhabdomyosarcoma cell line.* 2022.

Afzal, F., et al., *Detection of Uric Acid in UV-VIS wavelength Regime.* JOURNAL OF NANOSCOPE (JN), 2023. **4**(1): p. 75-81.

Ahmed, M., et al., *Review of Artificial Intelligence-based COVID-19 Detection and A CNN-based Model to Detect Covid-19 from X-Rays and CT images.* VFAST Transactions on Software Engineering, 2023. **11**(2): p. 100-112.

Asghar, S., et al., *Water classification using convolutional neural network.* IEEE Access, 2023. **11**: p. 78601-78612.

Batool, S.N. and G. Gilanie, *CVIP-Net: A Convolutional Neural Network-Based Model for Forensic Radiology Image Classification.* Computers, Materials & Continua, 2023. **74**(1).

Ghani, M. and G. Gilanie, *The IOMT-Based Risk-Free Approach to Lung Disorders Detection from Exhaled Breath Examination.* INTELLIGENT AUTOMATION AND SOFT COMPUTING, 2023. **36**(3): p. 2835-2847.

Gilanie, G., et al., *An automated and risk free WHO grading of glioma from MRI images using CNN.* Multimedia tools and applications, 2023. **82**(2): p. 2857-2869.

Hafeez, H.A., et al., *A CNN-model to classify low-grade and high-grade glioma from mri images.* IEEE Access, 2023. **11**: p. 46283-46296.

Khera, E.A., et al., *Characterizing nickel oxide thin films for smart window energy conversion applications: Combined experimental and theoretical analyses.* ChemistrySelect, 2023. **8**(37): p. e202302320.

Nazir, A., et al., *Exploring Breast Cancer Texture Analysis through Multilayer Neural Networks.* Scientific Inquiry and Review, 2023. **7**(3): p. 32-47.

Shafiq, H., et al., *Dental radiology: a convolutional neural network-based approach to detect dental disorders from dental images in a real-time environment.* Multimedia Systems, 2023. **29**(6): p. 3179-3191.

Ullah, H., et al., *Proteins and Triglycerides Measurement in Blood Under Ultraviolet (UV)/Visible (Vis) Spectroscopy at & lambda;= 190 to 1100 nm with an Additional He-Ne Laser Source.* LASERS IN ENGINEERING, 2023. **55**(3-6): p. 157-167.

Ullah, H., et al., *Assessing Graphene Oxide (GO) and CuO Nanocomposites for Effective Antibacterial Properties Using Laser Interferometry.* Lasers in Engineering (Old City Publishing), 2023. **55**.

Ullah, H., et al., *Early Detection of Liver, Ovary, Breast and Stomach Tumours in the Visible (λ= 630 nm) and Infrared (IR)(λ= 10.5 to 5.5 μm) Wavelength Regimes.* Lasers in Engineering (Old City Publishing), 2023. **54**.

Deppermann, K.L., et al., *Automated high-throughput seed sampler and methods of sampling, testing and bulking seeds*. 2017, Google Patents.

Xinshao, W. and C. Cheng. *Weed seeds classification based on PCANet deep learning baseline*. in *Signal and Information Processing Association Annual Summit and Conference (APSIPA), 2015 Asia-Pacific*. 2015. IEEE.

Gilanie, G., et al., *A Robust Method of Bipolar Mental Illness Detection from Facial Micro Expressions Using Machine Learning Methods.* Intelligent Automation & Soft Computing, 2024. **39**(1).

Naveed, S., et al., *Drug efficacy recommendation system of glioblastoma (GBM) using deep learning.* IEEE Access, 2024.

Rashid, M.S., et al., *Automated detection and classification of psoriasis types using deep neural networks from dermatology images.* Signal, Image and Video Processing, 2024. **18**(1): p. 163-172.

Saher, A., et al., *A Deep Learning-Based Automated Approach of Schizophrenia Detection from Facial Micro-Expressions.* Intelligent Automation & Soft Computing, 2024. **39**(6).

ULLAH, H., et al., *Potential application of CeO2/Au nanoparticles as contrast agents in optical coherence tomography.* Journal of Optoelectronics and Advanced Materials, 2024. **26**(July-August 2024): p. 307-315.

ULLAH, H., et al., *Measurements of Hyperproteinaemia in Human Blood Using Laser Interferometry: In Vitro Study.* Lasers in Engineering (Old City Publishing), 2024. **57**.

Adnan, M., et al., *ETHNICITY CLASSIFICATION FROM FACIAL IMAGES USING DEEP LEARNING METHODS.* Spectrum of Engineering Sciences, 2025. **3**(9): p. 1082-1156.

Ahmed, A., et al., *ADAPTING IPV6 AND 6LOWPAN OVER WIFI-BASED AODV MANETS FOR IOT APPLICATIONS.* Spectrum of Engineering Sciences, 2025. **3**(7): p. 1038-1052.

Akhtar, M., et al., *Harnessing optics and statistics for early detection and prognosis in breast and ovarian cancer.* Lasers in Medical Science, 2025. **40**(1): p. 279.

Amjad, M., et al., *Staging of Different Tumor by Utilizing Laser Guidance (@ 405 nm) in CT Scan Images Along with Statistical Analysis.* LASERS IN ENGINEERING, 2025. **59**(4-6): p. 309-325.

Amjad, M., et al., *Histopathology of Malignant Tissues Using High-Resolution Microscopy@ 630nm.* LASERS IN ENGINEERING, 2025. **59**(4-6): p. 295-308.

Anwaar, M., et al., *Optimizing Document Classification Using Modified Relative Discrimination Criterion and RSS-ELM Techniques.* International Journal of Advanced Computer Science & Applications, 2025. **16**(4).

Batool, S.N., et al., *Forensic Radiology: A robust approach to biological profile estimation from bone image analysis using deep learning.* Biomedical Signal Processing and Control, 2025. **105**: p. 107661.

Gilanie, G., et al., *A ROBUST CONVOLUTIONAL NEURAL NETWORK-BASED APPROACH FOR HUMAN EMOTION CLASSIFICATION: CROSS-DATASET VALIDATION AND GENERALIZATION.* Spectrum of Engineering Sciences, 2025. **3**(4): p. 782-798.

Gilanie, G., et al., *A ROBUST ARTIFICIAL NEURAL NETWORK APPROACH FOR EARLY DETECTION OF CARDIAC DISEASES.* Spectrum of Engineering Sciences, 2025. **3**(4): p. 499-511.

Gilanie, G., et al., *DEEP LEARNING-BASED APPROACH FOR ESTIMATING THE AGE OF PAKISTANI-GROWN RICE SEEDS.* Spectrum of Engineering Sciences, 2025. **3**(1): p. 557-572.

Gilanie, G., et al., *STEGANOGRAPHIC SECRET COMMUNICATION USING RGB PIXEL ENCODING AND CRYPTOGRAPHIC SECURITY.* Spectrum of Engineering Sciences, 2025. **3**(3): p. 323-336.

Gilanie, G., et al., *READABLE TEXT RETRIEVAL FROM NOISE-INFLUENCED DOCUMENTS USING IMAGE RESTORATION METHODS.* Spectrum of Engineering Sciences, 2025. **3**(3): p. 337-360.

Gilanie, G., et al., *PARAMETER OPTIMIZATION OF AUTOENCODER FOR IMAGE CLASSIFICATION USING GENETIC ALGORITHM.* Spectrum of Engineering Sciences, 2025. **3**(4): p. 201-213.

Kashif, A., et al., *FORENSIC RADIOLOGY: AN INTELLIGENT METHOD OF AGE AND GENDER ESTIMATION FROM X-RAY SCANNED BONES IMAGES USING CONVOLUTIONAL NEURAL NETWORKS.* Spectrum of Engineering Sciences, 2025. **3**(7): p. 440-487.

Latif, A., et al., *A VISION-FREE OBSTACLE DETECTION AND ALERT SYSTEM USING SMART KNEE GLOVES.* Spectrum of Engineering Sciences, 2025. **3**(6): p. 816-829.

Sajid, M., et al., *IoMT-Enabled Noninvasive Lungs Disease Detection and Classification Using Deep Learning-Based Analysis of Lungs Sounds.* International Journal of Advanced Computer Science & Applications, 2025. **16**(2).

Siddique, M.A., et al., *A Multi-Modal Approach for Exploring Sarcoma and Carcinoma Using FTIR and Polarimetric Analysis.* Microscopy Research and Technique, 2025.

Yang, J., et al., *BrainCNN: Automated Brain Tumor Grading from Magnetic Resonance Images Using a Convolutional Neural Network-Based Customized Model.* SLAS Technology, 2025: p. 100334.

Afzaal Akhtar, M., et al., *Deep Learning–Driven Automated Grading of Astrocytoma from Brain MRI Using an Enhanced DenseNet-169 Framework.* Computación y Sistemas, 2026. **30**(2): p. 1135.

Farooq, A., et al., *CONCEPTUAL FRAMEWORK FOR AN EEG-DRIVEN HUMAN BRAIN INTERFACE FOR NEURAL ENCODING AND DECODING.* Spectrum of Engineering Sciences, 2026. **4**(5): p. 2419-2435.

Farooq, A., et al., *A COLOR PRE-PROCESSING METHOD FOR TUMOR SEGMENTATION USING HUMAN LIVER CT IMAGES.* Spectrum of Engineering Sciences, 2026. **4**(6): p. 3159-3179.

Farooq, A., et al., *A NON-INVASIVE METHOD FOR BRAIN TUMOR DETECTION USING COMPUTER VISION AND DEEP LEARNING TECHNIQUES.* Spectrum of Engineering Sciences, 2026. **4**(6): p. 2575-2606.

Iqbal, M., et al., *Automated Identification of Mango Leaf Diseases Using Deep Convolutional Neural Networks.* Polish Journal of Environmental Studies, 2026.

Khursheed, A., et al., *A SMART HELMET TO DETECT ANOMALIES OF ITS USERS AND ENVIRONMENT.* Spectrum of Engineering Sciences, 2026. **4**(6): p. 399-418.

Khursheed, A., et al., *DEEP LEARNING-BASED COTTON PEST CLASSIFICATION USING COMPUTER VISION.* Spectrum of Engineering Sciences, 2026. **4**(6): p. 3869-3897.

Sajid, M., et al., *Internet of Medical Things-Driven Deep Learning Approach for Automated Heart Sound Classification.* IET Biometrics, 2026. **2026**(1): p. 3212328.

Yasir, M., et al., *Differentiation of metastatic and primary brain tumor using magnetic resonance imaging.* International Journal of Radiation Research, 2026. **24**(1): p. 259-265.

Kurtulmus, F., I. Alibas, and I. Kavdir, *Classification of pepper seeds using machine vision based on neural network.* International Journal of Agricultural and Biological Engineering, 2016. **9**(1): p. 51.

Kurtulmuş, F. and H. Ünal, *Discriminating rapeseed varieties using computer vision and machine learning.* Expert Systems with Applications, 2015. **42**(4): p. 1880-1891.